Engineering a Synthetic Microbial Consortium for Comprehensive Conversion of Algae Biomass like Terpenes for Advanced Biofuels and Bioproducts

SAND2015-8885J

Weihua Wu, Benjamin C. Wu, and Ryan W. Davis

Biomass Science & Conversion Technologies, Sandia National Labs, Livermore, CA

Abstract

Recent strategies for algae-based biofuels have primarily focused on biodiesel production by exploiting high algal lipid yields under nutrient stress conditions. However, under conditions supporting robust algal biomass accumulation, carbohydrate and proteins typically comprise up to ~80% of the ash-free dry weight of algae biomass. Therefore, comprehensive utilization of algal biomass for production of multipurpose intermediate- to high-value bio-based products will promote scale-up of algae production and processing to commodity volumes. Terpenes are hydrocarbon and hydrocarbon-like (C:O>10:1) compounds with high energy density, and are therefore potentially promising candidates for the next generation of value added bio-based chemicals and "drop-in" replacements for petroleum-based fuels. In this study, we demonstrated the feasibility of bioconversion of proteins into sesquiterpene compounds as well as comprehensive bioconversion of algal carbohydrates and proteins into biofuels. To achieve this, the mevalonate pathway was reconstructed into an *E. coli* chassis with six different terpene synthases (TSs). Strains containing the various TSs produced a spectrum of sesquiterpene compounds in minimal medium containing amino acids as the sole carbon source. The sesquiterpene production was optimized through three different regulation strategies using chamigrene synthase as an example. The highest total terpene titer reached 166 mg/L, and was achieved by applying a strategy to minimize mevalonate accumulation *in vivo*. The highest yields of total terpene were produced under reduced IPTG induction levels (0.25 mM), reduced induction temperature (25˚C), and elevated substrate concentration (20 g/L amino acid mixture). A synthetic bioconversion consortium consisting of two engineering *E. coli* strains (DH1-TS and YH40-TS) with reconstructed terpene biosynthetic pathways was designed for comprehensive single-pot conversion of algal carbohydrates and proteins to sesquiterpenes. The consortium yielded the highest total terpene yields (187 mg/L) at an inoculum ratio 2:1 of strain YH40-TS: DH1-TS, corresponding to 31 mg fuel/g algae biomass ash free dry weight. This study therefore demonstrates a feasible process for comprehensive algal biofuel production.

Keywords: algae biofuel, protein bioconversion, terpene biosynthesis, synthetic consortium, monoterpene, sesquiterpene, terpene synthase, bioproducts

Introduction

The need for sustainable, domestically produced replacements for petroleum has led to significant efforts for biofuels development[1]. Current carbon life cycle assessment suggests that production of biofuels from lignocellulosic and algae biomass provides up to ~50% GHG emission compared to petroleum[1-4]. Recent strategies for algae-based biofuels have primarily focused on biodiesel production through exploiting high algal lipid yields under the nutrient stress conditions. However, nutrient stress significantly compromises the overall biomass quantity and subjects the culture to increased susceptibility to contamination and subsequent culture crashes[5-7]. Under conditions supporting robust algal biomass accumulation, carbohydrate and proteins typically comprise up to ~80% of the ash-free dry weight of microalgae biomass[8-10]. Production of algal biofuel through comprehensive utilization of all of the biochemical components of algal biomass and the addition of high energy density fuel compounds with "fit for purpose" properties will both diminish the process cost and improve overall yield. A significant volume of research has been pursued to convert algal lipids and carbohydrates to biodiesel[11-13], ethanol[14-16], butanol[17], methane[18, 19], and isobutanol[20], however, little been reported regarding bioconversion of algal proteins. A recent work demonstrated the feasibility of converting algal protein to mixed short and medium chain fusel alcohols, such as isobutanol, 2-methy- and 3-methy-butanol, as well as other potentially high value alcohols, including phenylethanol, acetoin, and butanediol[21]. These medium chain alcohols present several benefits over ethanol, including >25% higher energy density, and dramatically lower hygroscopicity and corrosivity [22]. Despite the distinct advantages of these medium chain alcohols, the high oxygen content of these molecules makes them lack "fit for purpose" properties.

Isoprenoids, also referred to terpenes, are a group of natural products with over 55,000 structurally distinct chemical compounds. Compared to short and medium chain alcohols, these hydrocarbon and hydrocarbon-like (C:O > 10:1) compounds, including monoterpenes (C_{10}), sesquiterpene (C_{15}), diterpene (C_{20}) and their derivatives, not only have various biological functionalities but also contain higher overall energy density. In particular the sesquiterpene caryophyllene has been deemed to be among the top three most promising increased energy density jet fuel compounds[23]. Typically biologically derived fuel molecules have very high oxygen content (up to C:O of 2:1 for ethanol) introducing significant fuel cost and materials properties hurdles for blending into the petroleum-derived fuels infrastructure[24] . The near-zero oxygen content of terpene compounds in addition to their high energy density make them a particularly attractive candidate as "drop-in" fuel candidates for ground-based and aviation fuels. Terpenes also have a variety of higher value chemical applications,

e.g. as fragrances, flavoring agents, anti-fungi, and anti-virus, insect repellants, and pharmaceutical lead compounds[25-30]. However, few studies have reported means for conversion of biomass to terpene compounds. In this study, we demonstrate production of terpene compounds from high protein biomass composed of natural algae assemblages cultivated from wastewater in an Algal Turf Scrubber™ system[31]. Simultaneous conversion of the carbohydrate and protein fractions from the biomass was achieved using a synthetic microbial bioconversion consortium as a strategy for production of advanced biofuels and bio-based products.

Results

Terpene production from amino acids through mevalonate pathway reconstruction

In nature isoprenoids or terpenes are synthesized either by the mevalonate pathway (MEV)[32-35] or by the deoxy-D-xylulose 5-phosphate pathway (DXP)[36-38] in bacteria, fungi, plants and animals. In the mevalonate pathway, terpene biosynthesis starts with the condensation of two acetyl-CoA to produce acetoacetyl-CoA, in which acetyl-CoA is a critical niche in the central metabolism. Amino acids can be metabolized to form acetyl-CoA through pyruvate (Ala, Ser, Thr, Trp, Gly, Cys), through acetylacetate-CoA (Phe, Tyr, Trp, Lys, Leu), or through the TCA cycle (Pro Arg, His, Thr, Val, Ile, Met, Phe, Tyr). Given the fact of both pathways share common node: acetyl-CoA, it is possible to produce terpenes from protein lysate through metabolic engineering, as shown in figure 1. In this study, our synthetic biology strategy aimed to convert amino acids to high energy density and value-added terpene products through reconstruction of the terpene biosynthesis pathway into an *E. coli* chassis strain, YH40[21]. The enzymes in the mevalonate pathway diverted the metabolic flux from acetyl-CoA to the dimethylallyl pyrophosphate (DMAPP) and isopentenyl pyrophosphate (IPP) formation and further catalyzed by GPPS and TS to produce terpene. In our previous work, 12 novel terpene synthases were discovered through a synthetic biology platform[39]. Of the 12 novel terpene synthases, 6 were selected and sub-cloned downstream of the mevalonate pathway with truncated $GPPS_{Ag}$ (GenBank: AF513112.1) to demonstrate the feasibility of terpene production from protein.

Both monoterpene and sesquiterpene were detected from the culture of strains containing these six TSs when grown on M9 medium consisting of amino acids mixture as the sole carbon source (Table S1-S6). No terpene compounds were detected in the negative control strains. Among these six TSs, five of them produced sesquiterpene as the most abundant compounds in the culture headspace except TS-315006 which produced limonene (17.70% of total peak area) as the major product along with minor amounts of other sesquiterpene compounds: caryophyllene, chamigrene, valencene, pinene and others. Surprisingly, this TS was identified as τ-gurjunene synthase[39], which produced τ-gurjunene as the most abundant compound (accounting for 58.03% of total peak area) when the strain DH1-TS-315006 grew on EZ-rich medium and no obvious limonene was detected other than pinene. Compared to the host *E.coli* strain DH1, the strain YH40 is a derivative of *E.coli*

BW25113 and was specifically engineered to boost amino acid utilization[21]. The underlying reason that the major product was limonene instead of τ-gurjunene is yet unknown.

The YH40 strains containing TS-70183 and TS-6706 produced the widest spectrum of terpene compounds compared to the other four TSs. More than 15 terpene compounds were detected from cultures of each strain. The terpene compounds produced in the order of abundance were 1R,4R,7R,11R-1,3,4,7-tetramethyltricyclo[5.3.1.0(4,11)]undec-2-ene (6.8%), neoisolongifolene (4.9%), β-caryophyllene (2.0%), β-chamigrene (1.35%), and thujopsene-I3(1.0%). Comparison of the substrate dependence of the terpene profile of the TS-70183 containing strain indicated that although isoledene was the most abundant compound produced from glucose, this compound was not detected from culture on amino acids. Instead, 1R,4R,7R,11R-1,3,4,7-tetramethyltricyclo[5.3.1.0(4,11)]undec-2-ene (6.8%) was the major terpene product. Additionally, β-chamigrene and thujopsene-I3 were detected, which wasn't produced using a glucose-based fermentation broth. This product profile difference between two different carbon sources indicates that the TSs in two strains grown on two different media have different catalytic reaction mechanisms. The variation in the terpene profile was also observed for TS-6706 and other terpene synthases when the strains were grown on amino acids instead of glucose. TS-6706 was identified as caryophyllene synthase and yielded caryophyllene (40% of total peak area) as the most abundant compound when the strain was grown on glucose[39]. However, α-gurjunene was produced as the most abundant terpene compound (12.08% of total peak area) when grown on amino acids, followed by caryophyllene (10.42% of total peak area). Similar to DH1-6706 grown on glucose, YH40-6706 produced multiple sesquiterpene compounds as well as several monoterpene compounds. Compared to the caryophyllene synthase isolated from cotton[40] which yielded a small number of sesquiterpenes, the caryophyllene synthases in this study produced more than 20 sesquiterpene compounds as well as monoterpene compounds, indicating the complicated catalytic mechanism of the enzyme.

TS-322581 was identified as chamigrene synthase, which produced chamigrene as the major product when grown on glucose. Similarly, the strain YH40-322581 produced chamigrene as the most abundant terpene (43% of total peak area) when cultured on amino acids. Besides chamigrene, the additional monoterpenes limonene and pinene were also detected but with abundance less than 3.2% of total peak area. Compared to TS-6706, this enzyme tends to produce a single sesquiterpene compound, suggesting its distinct catalytic mechanism from TS-6706. For TS-80361 the three most abundant terpene compounds were β-chamigrene, β-caryophyllene, and (+)-valencene, indicating the enzyme is sesquiterpene synthase. Similar differences in the terpene profile were observed for this enzyme as well. In the previous study[39], TS-80361 was determined to be α-gurjunene synthase, which produced α-gurjunene as a major product from glucose with the monoterpenes pinene, limonene and its isomer as less abundant products. When grown on amino acids, however, the strain produced the three major sesquiterpene compounds mentioned above and monoterpenes were barely detected. TS-24646 was identified as α-selinene synthase[39], which produced α-selinene (50.7% of total peak area) as the most abundant compound from glucose. However, when cultured on protein as the sole carbon source, gurjunene was detected as the major product (21.2% of total peak area). Besides gurjunene, β-chamigrene and other monoterpenes such as

elemene, pinene and ocimene were also detected in the headspace of the culture, which is similar to the terpene profile from glucose.

Optimization of terpene production through different metabolic flux regulations

TS-322581 (chamigrene synthase) was chosen as a sample for metabolic flux optimization since this enzyme produces chamigrene as the sole sesquiterpene compound, making it straight-forward to evaluate and compare the end-product concentrations. To achieve the maximal metabolic flux to terpene production, three regulation strategies were designed and constructed, as shown in figure 2. In the first construct, all mevalonate pathway enzymes were cloned into one vector pJBEI3122 under two promoters with different strength. The first three enzymes (AtoB, HMGS, and HMGR) were cloned under the medium strength promoter lacUV5 and last four enzymes (MK, PMK, PMD, and idi) were expressed downstream of the strong promoter Ptrc to obtain maximal metabolic flux to GPPS. The signal peptide truncated $GPPS_{Ag}$ and chamigrene synthase were expressed into two separate plasmids under the strong promoters, T7 and Ptrc, respectively, to generate a large metabolic flux driving force toward the final products. These three plasmids were co-transformed into strain YH40 as an engineered host for terpene production. In the second construct, the $GPPS_{Ag}$ was cloned downstream of the enzyme idi under the Ptrc promoter in the plasmid pJBEI3122 to achieve the homologous expression of the intermediate pathway enzymes while the chamigrene synthase was expressed in a separate plasmid under strong promoter Ptrc. Both plasmids were co-transformed into strain YH40. In the third design, the $GPPS_{Ag}$ was cloned into the same plasmid with TS under the strong promoter Ptrc but ahead of the TS. The plasmid pJBEI3122 and plasmid-$GPPS_{Ag}$-TS were co-transformed into YH40. The strains containing different constructs were cultured in the M9 medium containing 20 g/L amino acids mixtures consisting of equal molar of each amino acid (Sigma, MO) to determine the terpene yield. Construct 1 produced the highest terpene concentration, up to 166.6 mg/L, comprised of 89.6 mg/L of monoterpene and 76 mg/L sesquiterpene (44 mg/L of chamigrene), followed by construct 3 (49 mg/L of total terpene) and construct 2 (31 mg/L of total terpene). Compared to construct 1 which produced higher monoterpene than sesquiterpene, the constructs 2 and 3 produced 3.8 and 2.7 fold higher concentrations of sesquiterpene than monoterpene. Interestingly, constructs 2 and 3 produced a lower amount of chamigrene than construct 1 but the percentage of chamigrene in sesquiterpene from construct 1 was the least (58%), compared to 85% and 94% from construct 2 and construct 3, respectively. To further elucidate the metabolic flux flow in the different constructs, the intermediate pathway metabolites were extracted and analyzed by the LC-MS. The results were consistent with the terpene concentrations obtained from the different regulation strategies. Only mevalonate accumulation was detected among all the intermediate metabolites and the concentrations were inversely related to the terpene yield. Construct 1 accumulated the least amount of mevalonate at 3.79 μM/g cell, followed by construct 3 (4.25 μM/g cell), and construct 2 (5.18 μM/g cell), respectively. The lower concentration of mevalonate suggests that higher metabolic flux was diverted to the product formation in construct 1 than in the other two regulation strategies. Additionally, mevalonate was

identified as the most likely toxic intermediate metabolite to cell growth[35, 41]. The consumption of mevalonate likely minimized toxicity, further improving the terpene production.

Optimization of inducer and amino acid concentration and fermentation temperature

The final terpene concentration is not only regulated by the transcriptional and translational rates but also by the thermodynamics of the pathway enzymes. IPTG was used as a common inducer for transcription of all of the terpene biosynthesis pathway genes in this work. The proper induction strength will optimize the transcriptional rate of pathway genes, which consequently results in the optimal enzyme concentrations that produce the maximum concentration of the target terpene compounds. From the experimental results, 0.25 mM of IPTG yielded the highest total terpene concentration, up to 140 mg/L, including 64 mg/L monoterpene and 75 mg/L sesquiterpene, as shown in figure 3. The strain induced at 0.5 mM IPTG produced 91 mg/L of total terpene, which was about 36% less than that produced at 0.25 mM IPTG. The similar concentrations of total terpene were detected when the strains were induced at 1mM and 1.5 mM, which were ~53% of the total terpene produced when induced by 0.25 mM IPTG. Substrate inhibition is believed to be a significant factor affecting product yield during fermentation[42]. The substrate of amino acid mixture contains charged amino acids (Arg, Lys, Asp, Glu) and other polar amino acids. The high concentration of amino acids in the fermentation medium may increase the ionic strength of the medium resulting in the low cell growth. Therefore, the effects of amino acid concentration on terpene yield were also investigated in the study. The results showed that the terpene yield increased with the elevation of the amino acid concentration in the medium, as shown in figure 3B. At 20 g/L amino acids, the strain produced the highest terpene titer, up to 166.6 mg/L total terpene while only 18 mg/L of total terpene was produced when the medium contained 5 g/L amino acids. Contrarily, the ratio of sesquiterpene to monoterpene was the highest in the culture on 5 g/L amino acids, up to a factor of ~5. This ratio decreased with increasing amino acid concentrations in the medium. At 20 g/L amino acid, the strain produced more monoterpene than sesquiterpene. The reason of the terpene profile shift is not clear. The concentration of the terpenes produced is dependent on the reaction rate, which is determined by the properties of pathway enzymes, their concentrations, and the reaction temperature. According to the Arrehenius equation, the chemical reaction rate increases with the temperature increase. However, in terms of the enzymatic reaction, there exists an optimal reaction temperature at which the enzyme has maximal catalytic ability. Based on the experimental results, the terpene concentration reached the highest value when the strain was induced at 25˚C, up to 71 mg/L. When the induction temperature rose to 30˚C and 37˚C, the strain produced only 28% (20 mg/L) and 21% (15 mg/L) of the terpene yielded at 25˚C. The strain produced only very small quantities of terpene at 42˚C.

Comprehensive utilization of algal carbohydrate and protein for terpene production

It is commonly speculated that in an algae for fuels process, the algal carbohydrate will be bio-converted into ethanol and algal proteins will be utilized as animal feeds or other non-fuel applications[15, 20, 43, 44].To improve the technoeconomic feasibility of algae for fuels, it is necessary to improve the algal biofuel processing

options by the addition of intermediate-value petroleum replacements and fuel compounds which are compatible with current fuel engine infrastructure. With a deliberately designed microbial consortium, we successfully demonstrated the simultaneous fermentation of algal carbohydrates and proteins into terpene compounds as a next generation fuel concept, as illustrated in figure 4. The terpene biosynthetic pathway was constructed in *E.coli* strains YH40 and DH1. The strain YH40-TS was designated to convert algal protein into terpene while DH1-TS was designed to consume the carbohydrate for terpene formation. The terpene yield was investigated under three different combinations of inoculum YH40-TS/DH1-TS at the ratio 2, 1, 0.5 as well as the single strain YH40-TS or DH1-TS only. The experimental results showed that the terpene yield reached 187 mg/L total terpene at the ratio of 2 (YH40-TS/DH1-TS), including 87 mg/L of monoterpene and 100 mg/L of sesquiterpene, in which the chamigrene was the major product accumulated up to 62 mg/L. The synthetic microbial consortia produced similar total terpene at the ratio of 1 and 0.5 (YH40-TS/DH1-TS), which were ~150 mg/L of total terpene. The microbial consortium at ratio1 yielded the highest concentration of sesquiterpene (113 mg/L) as well as chamigrene (80 mg/L) among three consortia while the monoterpene yield was the lowest (34.5 mg/L). The strains YH40-TS and DH1-TS alone only produced 26 and 43 mg/L of total terpene, respectively, indicating relatively inefficient bioconversion of algal biomass. Compared to single strain, the synthetic microbial consortia produced 2.5-6.2 times higher total terpene concentration, suggesting that both algal carbohydrate and protein can be more effectively converted in the single-pot process. In terms of algal carbohydrate and amino acid consumption, none of the synthetic consortia were able to completely consume the algal carbohydrates and amino acids. The 2:1 consortium ratio utilized the highest amount of algal biomass, corresponding to 36.8% of total carbohydrates and 31.3% of algal amino acids. The other two consortia ratios consumed similar amount of the total carbohydrates and algal amino acids, which were 10-15% less than the 2:1 consortium. Strain YH40-TS utilized approximately half of the algal amino acids in the medium but algal carbohydrate consumption was minimal (3.8% of total carbohydrate). Strain DH1-TS consumed both algal carbohydrates (37.8 % of total carbohydrate) and amino acids (23.3% of algal amino acids) in the medium. In our previous algal composition analysis, carbohydrate and protein accounts for 74.2% of Hydromentia ATS™ algal biomass ash free dry weight. Based on this data, the 2:1 consortium ratio produced the highest terpene yield at 30.5 mg terpene/ g algae while the 1:1 and 1:2 consortium ratios yielded 27.0 and 28.5 mg terpene/ g algae, respectively. The strain YH40-TS only produced 3.3 mg terpene/ g algae, which was lower than 8.7 mg terpene/ g algae yielded by strain DH1-TS, as shown in figure 4.

Discussion

First generation biofuels encountered severe criticism because the feedstocks are common food crops, which raised concerns about global food security, especially with regards to the most vulnerable regions of the global economy. As recently reviewed[4, 9, 10, 15, 44, 45], microalgae-based biofuels have been become recognized as an important feedstock for second generation biofuels in addition to lignocellulosic biomass. Techno-economic

analysis suggests that a viable algal biofuel process will require high algae biomass productivity, inexpensive harvesting and biomass pretreatment methods, as well as co-production of high value products in addition to conventional fuel compounds such as ethanol and diesel [9, 10, 24]. Leveraging the development of high value products, such as terpenes, with the comprehensive utilization of algae biomass through heterotrophic fermentation has several advantages in terms of process cost reduction[24]. Terpenes as hydrocarbon or hydrocarbon-like compounds have only recently been considered as a next generation fuel[46-50]. Via photosynthetic pathways, algae microorganisms are able to produce large amount of protein(~40-60%) , carbohydrates (~25-40%) , and lipid (~10-20%) under non-stressed conditions [9, 10]. Therefore, efficient utilization of algae biomass for conversion to fuels requires processes to convert both of the major algal biochemical pools (proteins and carbohydrates) to high energy density and low oxygen liquid fuels to support algal biofuel process viability and generation of effective petroleum replacements.

Efficient conversion of algal proteins and carbohydrates to terpene compounds at high yields is of critical importance for economically feasible algal biofuel process. For terpene production, biosynthesis can be achieved either through the mevalonate or DXP pathways, for which the metabolic flux is diverted from acetyl-CoA and pyruvate, respectively, to the final products[41, 51-54]. Correspondingly, both carbohydrate and amino acid assimilation can yield pyruvate and acetyl-CoA as common building blocks in the central metabolism although the catabolism of amino acids has more diverse pathways than that of glucose, as shown in the figure1. These facts enable terpene production through comprehensive utilization of algal carbohydrates and proteins with a deliberately designed synthetic microbial consortium. In this study, algal carbohydrate and proteins from natural benthic algal polyculture (ATS™ biomass provided by Hydromentia, Inc) was effectively converted to the sesquiterpene chamigrene as well as several monoterpene compounds. The highest total terpene yield from shaker flask experiments was up to 187 mg/L, corresponding to ~30.6 mg terpene/ g algae. The low terpene yield is due to several factors. First of all, the ATS™ biomass contained elevated inorganic loading, which resulted in high ionic strength and osmotic pressure in the fermentation medium and likely caused inhibition of cell growth and subsequent terpene formation. Furthermore, strain DH1-TS is limited to conversion of hexose and several amino acids, while YH40-TS can utilize 13 amino acids but has low efficiency uptake of algal carbohydrates. However, the pretreated algal biomass contains both hexose and pentose as well as all of the 20 amino acid variants. The incomplete algal carbohydrate and amino acids consumption capability further diminished the terpene yield. Additionally, the minimal medium of fermentation only contains pretreated algal carbohydrate and protein as which may lack cofactors for terpene biosynthesis pathway enzymes and other essential functional proteins.

In terms of the potential for terpene yield improvement, terpene biosynthesis is limited by transcriptional and translational regulation as well as the enzyme kinetics or reaction thermodynamics they catalyze. To optimize the expression of proteins in the mevalonate pathway and generate the optimal metabolic flux to the desired final products, all the pathway genes were expressed under the control of different promoter combinations with different transcriptional and translational regulations. In construct1, the first three enzymes of MEV pathway

(AtoB, HMGS, and HMGR) were regulated under a medium strength promoter LacUV5 to achieve the medium level of mevalonate accumulation, which was able to minimize the toxicity of mevalonate to cell growth. While the last four enzymes (MK, PMK, PMD, and IDI) were expressed under strong promoter Ptrc to divert maximal flux to the IPP and DMAPP as well as to efficiently consume the toxic intermediate metabolite mevalonate[33, 35, 43, 55]. Additionally, to drive the resulting metabolic flux to the final terpene products, both downstream enzymes $GPPS_{Ag}$ and chamigrene synthase were over-expressed under strong promoters T7 and Ptrc, respectively. From our shaker flask experiments, the strain containing construct 1 yielded ~166.6 mg/L total terpene, including 89.6 mg/L monoterpene and 76 mg/L sesquiterpene with chamigrene as the major product. Compared to construct 1, both construct 2 and construct 3 have less transcriptional and translational efficiency of downstream enzymes including $GPPS_{Ag}$ and chamigrene synthase, indicated by higher mevalonate levels *in vivo* which diminished the cell growth as well as the final terpene yields. IPTG was employed as a common inducer for the LacUV5, T7, and Ptrc promoters to initiate protein expression and subsequent catalysis of the metabolic reactions to terpene generation. The concentration of the IPTG was optimized for maximal terpene production. At low concentrations of IPTG (0.25 mM), the strain yielded the highest terpene concentration, up to 140 mg/L. The terpene yield decreased with elevation of the IPTG concentrations. The decreased terpene yield at higher induction levels in this study is likely due to the different induction efficiencies of promoters LacUV5, T7, and Ptrc, which may result in induction competition[56, 57] among the different promoters that further leads to the imbalance of the metabolic flux resulting in reduced product yield. Additionally, at high concentrations IPTG is toxic to cell growth, which further compromised the terpene formation. The terpene yield is also subject to the fermentation environmental factors, such as temperature and substrate concentration. The strain YH40-TS produced higher terpene yield at lower temperature and produced negligible terpene quantities at 42°C. Most likely this is because the lower temperature initiated the optimal translation rate of terpene pathway enzymes to achieve optimal fully functional pathway enzymes concentrations *in vivo,* which catalyzed the maximum metabolic flux to the terpene formation[58]. The terpene yield may also be subject to the effect of substrate inhibition during the fermentation. In this experiment, the terpene yields on amino acid concentrations above 20g/L were not investigated due to the limited solubility of amino acids, especially those with aromatic side chains. Within the concentration range of 5- 20g/L amino acids, the terpene yields increased with higher amino acid concentrations. The reason for the increased terpene yield is probably due to the fact that the amino acids were the only carbon source in the medium. At the low concentration of amino acids, the strain utilized the majority of amino acids for cell growth and maintenance instead of terpene production.

Regarding the multiple terpene products yielded from each strain, all six selected TSs are type I terpene cyclase, containing two highly conserved motifs: the aspartate rich motif (DDXXD) and the NSE triad (ND(L/I/V)XSXXXE)[59, 60] which is involved in substrate precursors (GPP, FPP) binding and catalyzing terpene formation. The general mechanism of monoterpene formation starts from the ionization of geranyl diphosphate to form geranyl cation followed by isomerization to several different carbocations. The resulting carbocations undergo a range of cyclization, hydride shifts, methyl shifts, and conformation rearrangements before the

reaction is quenched by deprotonation or water capture[60-62]. The mechanism of sesquiterpene formation is similar to monoterpene but with higher complexity due to the higher complexation state of FPP than that of GPP, which involves multiple isomerations of carbocations and cyclization reactions[60-62]. The different intermediate carbocations can undergo different cyclization reactions, hydride or methyl shifts, and conformation rearrangements which is most likely the reason of multiple products formation from each terpene synthase. Additionally, the product profile is not only determined by the catalyzing properties of terpene synthase but also the reaction environment since the reaction is also terminated by deprotonation or water capture. The strains YH40-TSs were grown on the M9 medium containing a mixture of amino acids which has higher ion strength and lower pH than that of EZ-rich medium. This may explain the terpene profile of the same TS is different from two different growth media.

Conclusion

Algae-based biofuels production has primarily focused on biodiesel production through transesterification of algal lipids. Under robust algal biomass accumulation conditions, carbohydrate and proteins typically comprise up to ~80% of the ash-free dry weight of algae biomass. Therefore, a comprehensive process for bioconversion of algal carbohydrates and proteins to high energy density fuels and value-added bioproducts should significantly improve the algal fuel process feasibility. In this study, we demonstrated simultaneous bioconversion of algal carbohydrates and proteins to terpenes which are attractive candidates for high energy density aviation fuels and other intermediate to high value biobased chemicals applications. Using an engineered microbial consortium, greater than 30% of the carbohydrates and proteins from a wastewater-based mixed algal feedstock were converted to terpenes, including both monoterpenes and sesquiterpenes. This microbial consortium concept for comprehensive utilization of algal biomass offers a versatile path forward for the production of fuels and active bioproducts from algae.

Material and Methods

Stains and Plasmids

The mutant *E.coli* strain YH40 (BW25113/F' [traD36, proAB+, lacIqZΔM15]ΔglnA, ΔgdhAΔluxSΔlsrA) was generously provided by Professor James C Liao from University of California, Los Angeles (UCLA)[21]. The plasmids pJBEI3122, pBbE1a, and pBbE2k were provided courtesy of Dr. Jorge Alonso-Gutierrez from the Joint BioEnergy Institute (JBEI). The plasmid pJBEI3122 contains the mevalonate pathway genes encoding seven enzymes[63] (AtoB, HMGS, HMGR, MK, PMK, PMD, and IDI) except the geranyl diphosphate synthase (GPPS) and terpene synthase (TS). All six selected terpene synthase gene and the GPPS gene (GenBank: AF513112.1, $GPPS_{Ag}$) from

Abies grandis with the chloroplast signal peptide truncated were codon optimized based on *E.coli* codon bias. The Ribosome Binding Site (RBS) for each terpene synthase gene was created and optimized by online RBS calculator developed by Dr. Salis Lab[64]. All the gene sequences containing RBS site and restriction enzyme cutting sites were synthesized by Genscript.

Reconstruct the terpene synthetic pathway into *E.coli* strain YH40

Each synthesized terpene synthase and $GPPS_{Ag}$ ORF including the sequences of corresponding ribosome binding site was sub-cloned into plasmid pBbE1a and pBbE2K, respectively, under *EcoR*I and *BamH*I cutting site to obtain vector pBbE1a-TS and pBbE2K-$GPPS_{Ag}$as described before[39]. The plasmids pJBEI3122, pBbE1a-TS, and pBbE2k-$GPPS_{Ag}$ were co-transformed into expression host YH40 for the terpene production. The plasmids pJBEI3122 and pBbE2k-$GPPS_{Ag}$ were co-transformed into strain YH40 as negative control as well.

The gene $GPPS_{Ag}$ was amplified (Primer 1: 5-GTG TGG AAT TGT GAG CGG ATA AC-3, Primer-2: 5-GGA TCC CTC GAG TCA ATT TTG TCT GAA TGC CAC G-3) from the vector pBbE2K-$GPPS_{Ag}$and subcloned into plasmid pJBEI3122 right downstream of gene isoprenyldiphosphate isomerase (*idi*), under the restriction cutting site *Bgl*II and *Xho*I, to obtain plasmid pJBEI3122-$GPPS_{Ag}$. Additionally, the amplicon of gene $GPPS_{Ag}$ was sub-cloned, under *EcoRI* cutting site, into plasmid pBbE1a-TS to obtain plasmid pBbE1a-$GPPS_{Ag}$-TS. The right orientation of gene $GPPS_{Ag}$ was confirmed by diagnostic PCR using primer 3 (5-CAT CCG GCT CGT ATA ATG TGT GG-3) and primer 4 (5-GCTC CTC GGT TCC TCC AAC AAG-3). The plasmid pJBEI3122-$GPPS_{Ag}$ and pBbE1a-TS, pJBEI3122 and pBbE1a-$GPPS_{Ag}$-TS, were co-transformed into both *E.coli* strain DH1and YH40 for the terpene production

Production of the terpene compounds by the engineered *E.coli* strain

The transformants containing each terpene synthase were cultured in 15 ml of LB medium with 100 μg/L of ampicillin, 34 μg/L cholorphenicol, and 25 μg/L of kanamycin. The cultures were incubated at 37˚C at 220 rpm overnight. Then, 15 ml of the overnight culture was centrifuged. The cell pellets were re-suspended twice into 4 ml of 1xM9 medium[65] and inoculated into 30 ml of 1X M9 containing 20 g/L amino acid mixture (Sigma, MO) as the sole carbon source. The culture was incubated at 37˚C, 220 rpm until the OD_{600nm} reached 0.8 and then terpene production was induced by adding isopropyl-β-D-1-thiogalactopyranoside (IPTG) at the final concentration 1mM. The flasks were cap-sealed and cultured for another 72 hours at 30˚C, 200 rpm to allow terpene accumulation.

Terpene production from a synthetic consortium of *E.coli* strains (DH1-TS and YH40-TS)

ATS™ biomass samples were pretreated according to protocols from the National Renewable Energy Laboratories and hydrolyzed with 2 mg/L Pronase (promega, CA) following the manufacturer's protocol. The pretreated and hydrolyzed algal biomass was sterilized through filtration. *E. coli* strains DH1 and YH40 each

containing the terpene biosynthesis pathway were cultured into 15ml of LB medium as described above. The overnight cultures were centrifuged and the cell pellets were re-suspended into 4 ml of pretreated ATS™ biomass hydrolysate. Various ratios (2:1, 1:1, 1:2) of YH40-TS to DH1-TS were inoculated into the algal hydrolysate at a final concentration of 10% v/v. The culture were incubated at 37˚C, 220 rpm and induced with 0.25 mM IPTG once the OD reached 0.8. The flasks were cap-sealed and cultured for another 72 hours at 25˚C, 180 rpm for terpene production. Analytical samples were taken at the initial and end point of fermentation. The concentrations of total carbohydrate and amino acids were determined according to the established colorimetric protocols.

Terpene analysis by GC/MS and metabolite analysis by LC-MS

The terpene compounds in the headspace were extracted with a preconditioned solid-phase micro-extraction (SPME) syringe consisting of 50/30 divinylbenzene/carboxen on polydimethylsiloxane on a Stable Flex fiber as described previously[39]. The SPME fiber was inserted into the headspace of each culture flask for 30 minutes to absorb the terpene compounds. Volatile terpene compounds absorbed to the SPME fiber were analyzed by GC-MS (Varian 3800) containing a 30mm x0.25mm i.d. DB wax capillary column with a film thickness 0.25 μm, as described in a previous study[39]. The column was temperature programmed as follows: 60˚C for 4 min, increasing to 120˚C at 10˚C/min and holding for 5 min, then increasing to 220˚C at 20˚C/min and holding for 2 min, then increasing to 250˚C at 50˚C/min and holding for 4 min. The carrier gas was ultra-high purity helium at a constant flow rate of 1 ml/min. A two minutes injection time was used to desorb the terpene compounds from the sampling fiber into a splitless injection (220˚C) of the chromatograph coupled with a Saturn 2000 ion trap mass spectrometer. The MSD parameters were EI at 70eV, mass range was 30-500 Da, and the scan speed was 2 scans/sec. Spectral components were searched against the NIST 2011 mass spectral library , and only components with mass spectra match factors > 85% were reported as tentatively identified compounds. Compounds with peak areas > 1% of the total peak area in the chromatogram are reported.

24 hours after induction, cultures were centrifuged at 14000 rpm for 10 mins, and rinsed with cold DI water three times. Cell pellets were resuspended with 1 ml of methanol and placed in a bead beater apparatus for two rounds of cell disruption at 4˚C to completely break down the cells. The mixture was centrifuged and the supernatant were transferred to new 2 ml vials. 750 μl of DI water was added into sediment lysate and vortexed vigorously at 4˚C. The supernatant was then combined with methanol extract, the methanol in the mixture was blow off by N_2 gas, and the leftover mixture was filtrated through a 3KDa MWCO spin column (Millipore). The metabolites were analyzed using LC-MS according to the method of Rodrigues et al[66].

Estimation of terpene titer in the culture

A serial dilution of pinene, limonene, and caryophyllene were added into the same amount of culture media with inoculum of negative control strain to simulate the liquid-gas phase balance of terpene compounds produced in the culture. The flasks were sealed and incubated under same conditions as terpene formation

strains. The terpene compounds in the headspace were collected by SPME as described above. The adsorption time was carefully optimized to make sure the fibers were not saturated and the amounts of absorbed terpene compounds were in the linear regression relationship for the standard curve. The same adsorption time were applied for all the cultures. The concentrations of terpene compounds produced in the culture were calculated through referring to the standard curve.

Acknowledgments: The authors would like to thank Mark J. Zivojnovich, VP of Project Development at HydroMentia, Inc. for providing ATS™ algae biomass samples for this effort. We would also like to thank Prof. James Liao, Chair of the Department of Chemical and Biomolecular Engineering at UCLA for providing the *E. coli* YH40 strain and helpful discussions regarding conversion optimization. Special thanks to Jay Keasling, Taek-Soon Lee, and Jorge Alanzo-Gutierrez for providing strains and giving advice on expressing TS and Dr. Edward Baidoo for help with LC-MS analysis. Sandia is a multi-program laboratory operated by Sandia Corporation, a Lockheed Martin Company, for the United States Department of Energy under Contract DE-ACO4-94AL85000. Support is acknowledged from DOE-EERE BioEnergy Technologies Office (BETO) under agreement number 26336.

Caption of Figures and Tables

Figure 1: Amino acid assimilation connects to the isoprenoid biosynthesis pathway through acetyl-CoA[21, 52]

Figure 2: Optimization of terpene production through different pathway enzyme regulation strategies. A: Construct 1: GPPS and TS were expressed in separate plasmids under strong promoters, mevalonate pathway enzymes were expressed under medium strength promoter LacUV5 and strong promoter Ptrc, respectively, to optimize flux to GGP; Construct 2: mevalonate pathway enzymes and $GPPS_{Ag}$ were expressed under medium strength promoter LacUV5 and strong promoter Ptrc, respectively, to optimize flux to GGP, TS was regulated by a strong promoter T7; Construct 3: $GPPS_{Ag}$ and TS were tandem expressed under a strong promoter Ptrc, mevalonate pathway enzymes were expressed under medium strength promoter LacUV5 and strong promoter Ptrc, respectively, to optimize flux to GGP. B: Terpene concentrations produced from different constructs. C: *in vivo* metabolite mevalonate concentrations under different regulation strategies

Figure 3: Optimization of the terpene formation from construct 1. A: Induction with different concentrations of IPTG, B: Terpene production in construct 1induced with 0.25 mM IPTG under variable amino acid concentrations, C: Terpene formation in construct 1 induced with 0.25mM IPTG under variable temperature.

Figure 4: Comprehensive conversion of algal carbohydrate and protein into terpenes using synthetic microbial consortia. A: terpene production using a microbial consortium under variable inoculum ratios, B: Substrate consumption and terpene yield of the microbial consortium under variable inoculum ratios.

Table S1: Terpene compounds produced from the engineered strain, YH40-322581

Table S2: Terpene compounds produced from the engineered strain, YH40-315006

Table S3: Terpene compounds produced from the engineered strain, YH40-70183

Table S4: Terpene compounds produced from engineered strain, YH40-80361

Table S5: Terpene compounds produced from the engineered strain, YH40-24646

Table S6: Terpene compounds produced from the engineered strain, YH40-6706

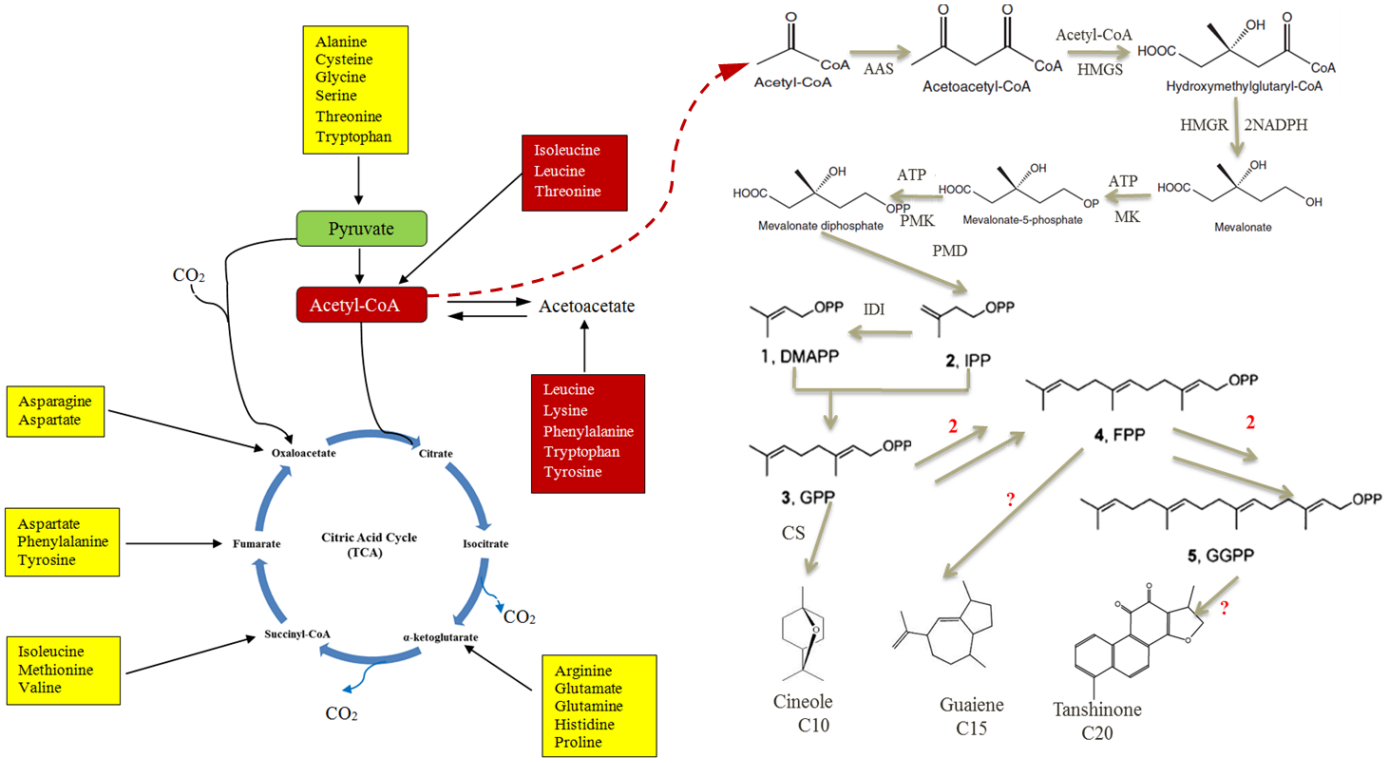

Amino Acids Assimilation

Terpene Biosynthesis Pathway

Figure 1

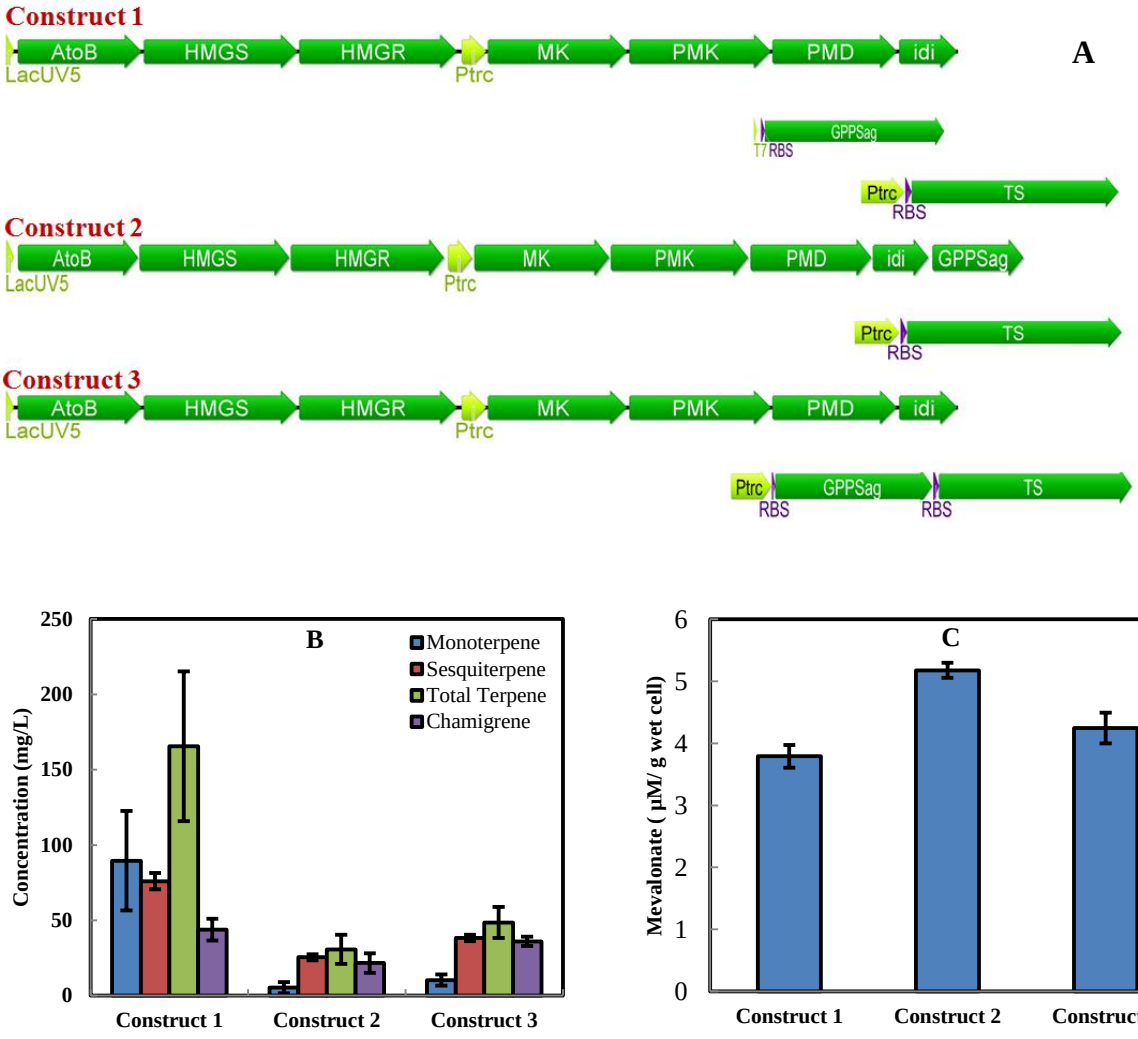
Construct 1
AtoB
HMGS
HMGR
MK
PMK
PMD
idi
LacUV5
Ptrc
A
GPPSag
T7
RBS
Ptrc
TS
RBS
Construct 2
AtoB
HMGS
HMGR
MK
PMK
PMD
idi
GPPSag
LacUV5
Ptrc
Ptrc
TS
RBS
Construct 3
AtoB
HMGS
HMGR
MK
PMK
PMD
idi
LacUV5
Ptrc
Ptrc
GPPSag
TS
RBS
RBS
B
Monoterpene
Sesquiterpene
Total Terpene
Chamigrene
Concentration (mg/L)
250
200
150
100
50
0
Construct 1
Construct 2
Construct 3
C
Mevalonate (µM/ g wet cell)
6
5
4
3
2
1
0
Construct 1
Construct 2
Construct 3

Figure 2

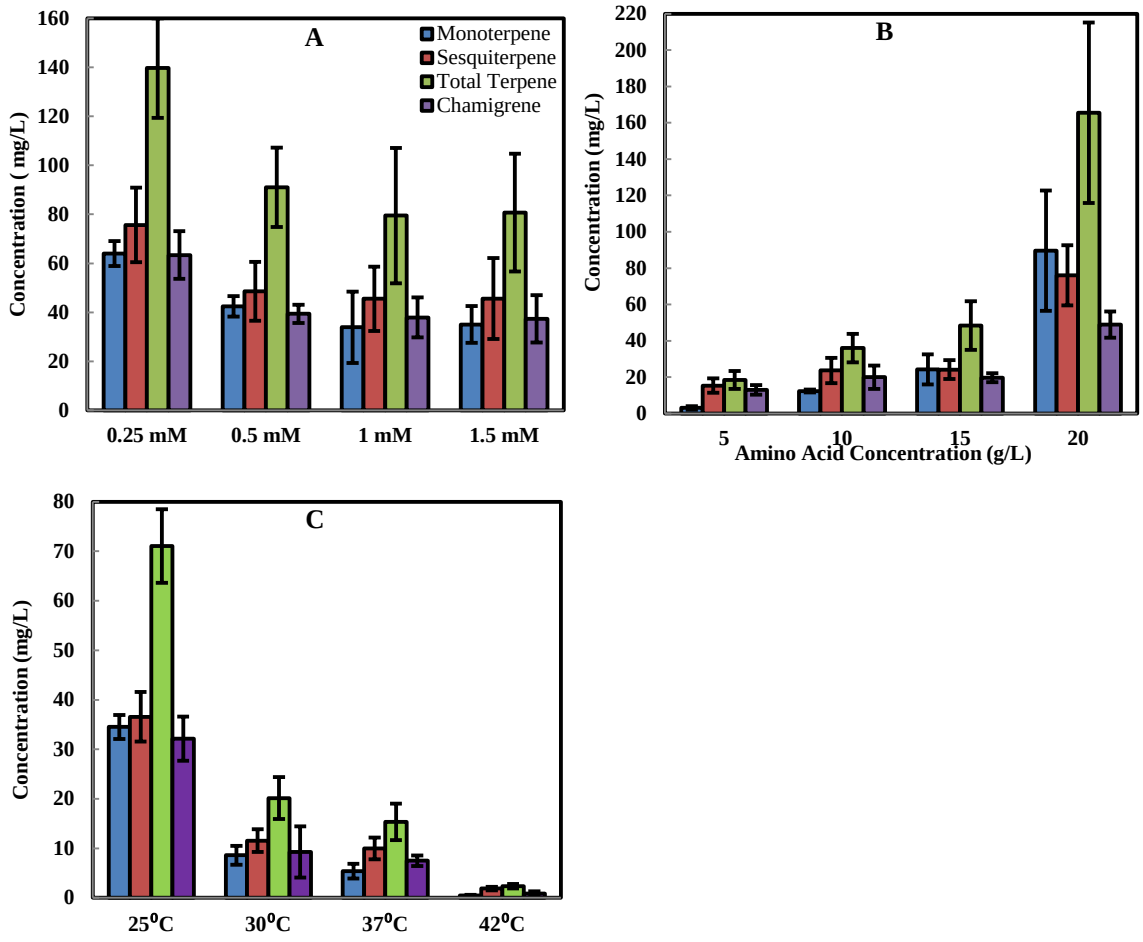
A
Monoterpene
Sesquiterpene
Total Terpene
Chamigrene
Concentration (mg/L)
0.25 mM
0.5 mM
1 mM
1.5 mM
B
Concentration (mg/L)
Amino Acid Concentration (g/L)
C
Concentration (mg/L)
25°C
30°C
37°C
42°C

Figure 3

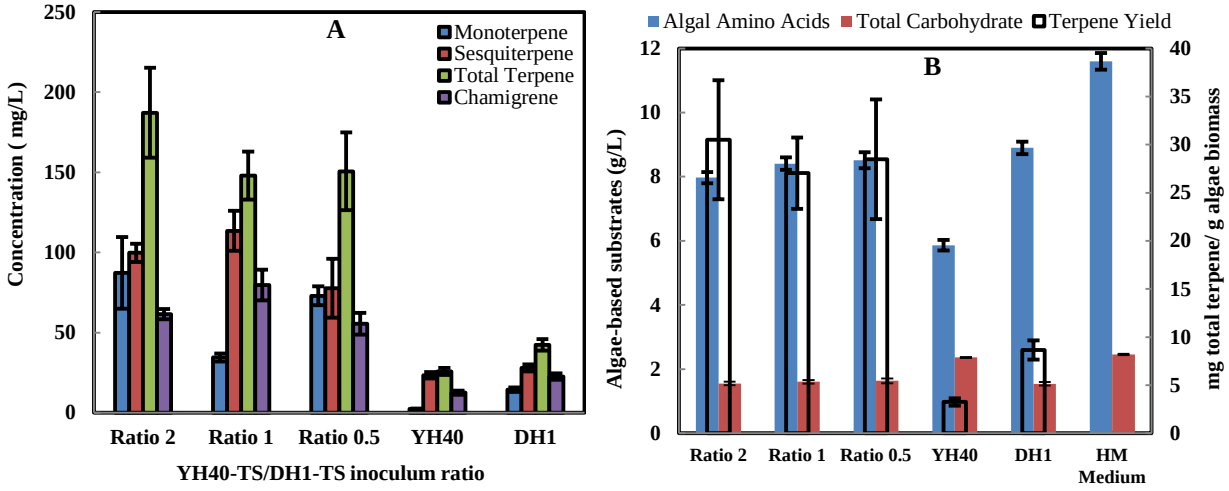
A
Monoterpene
Sesquiterpene
Total Terpene
Chamigrene
Concentration (mg/L)
250
200
150
100
50
0
Ratio 2
Ratio 1
Ratio 0.5
YH40
DH1
YH40-TS/DH1-TS inoculum ratio
Algal Amino Acids
Total Carbohydrate
Terpene Yield
B
Algae-based substrates (g/L)
12
10
8
6
4
2
0
40
35
30
25
20
15
10
5
0
mg total terpene/ g algae biomass
Ratio 2
Ratio 1
Ratio 0.5
YH40
DH1
HM Medium

Figure 4

Supplemental Tables:

Table S1:

YH40-322581 on Amino Acids					
Compound	Retention Time (min)	% total peak area	Match (%)	R-match (%)	Peak ID
beta-chamigrene	18.518	43.135	89.5	91.4	f
Limonene	8.777	3.145	92.3	92.5	b
beta-pinene	8.067	2.518	94.4	94.7	a
Eremophila-1(10),11-diene	18.663	1.051	94.2	95.8	g
p-cymene	10.018	0.691	95.5	97.5	d
τ-terpinene	9.581	0.469	89.1	95.6	c
4-Methyl-3-(1-methylethylidene) -1-cyclohexene	10.203	0.395	92.9	95.9	e

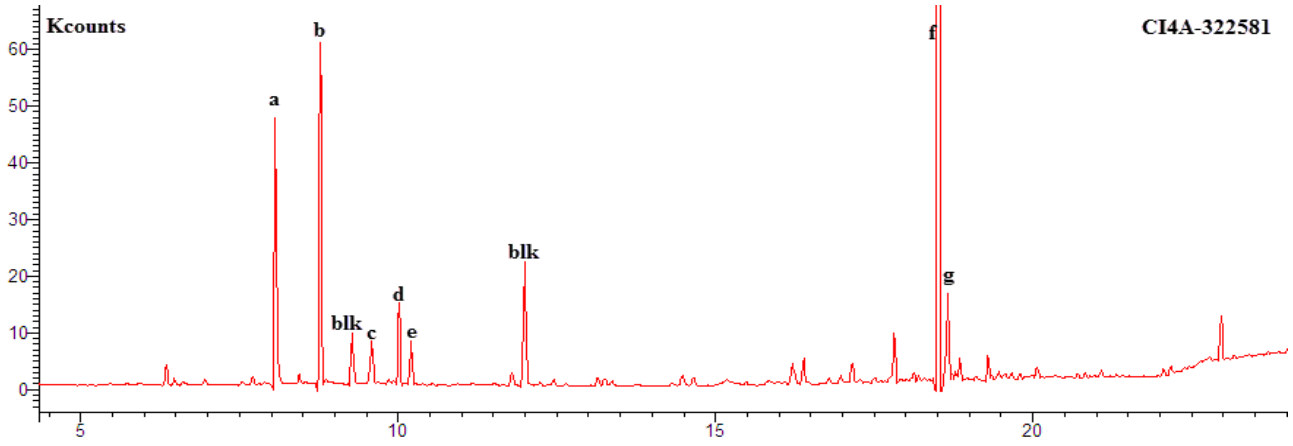

Table S2:

YH40-315006 on Amino Acids					
Compound	Retention Time (min)	% total peak area	Match (%)	R-match (%)	Peak ID
limonene	8.759	17.701	91.5	91.6	b
caryophyllene	17.319	2.768	95.2	96.1	l
beta-chamigrene	18.547	1.82	88.9	90.1	f
(+)-valencene	18.701	1.508	95.2	96.1	m
butylated hydroxytoluene	20.121	1.303	91.3	92.6	n
beta-pinene	8.038	0.971	89.2	93.8	a
1R-*alpha*-pinene	5.428	0.927	93.2	96.9	j
Ethyl propanoate	4.26	0.86	88.7	92.2	i
1,3,5-cycloheptatriene	5.879	0.38	86.4	93.8	k

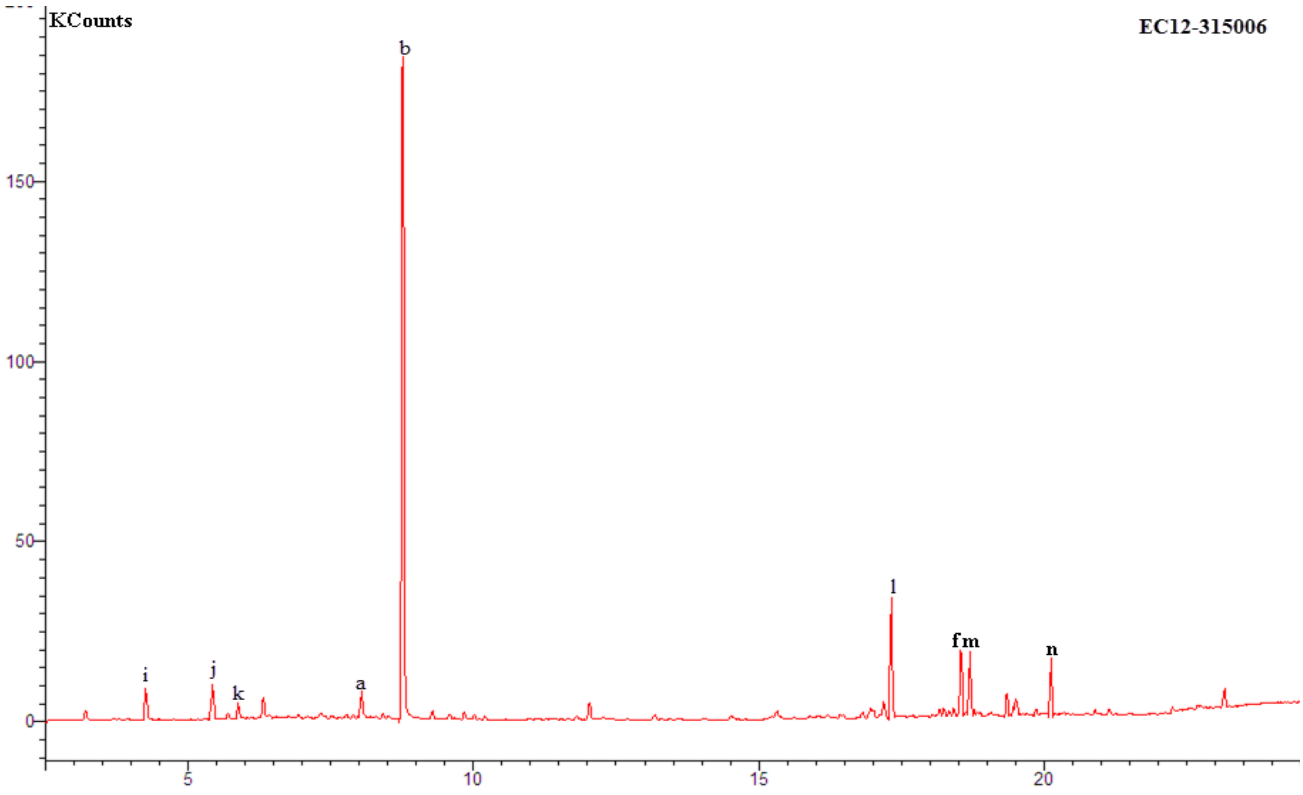

Table S3:

YH40-70183 on Amino Acids					
Compound	Retention Time (min)	% total peak area	Match (%)	R-match (%)	Peak ID
1R,4R,7R,11R-1,3,4,7-Tetramethyltricyclo [5.3.1.0(4,11)]undec-2-ene	15.396	6.781	84.2	86.6	x
Neoisolongifolene	12.848	4.874	89.6	90.5	s
β-caryophyllene	17.321	2.008	94.5	95.5	l
β-chamigrene	18.551	1.345	89.9	90.8	f
Thujopsene-I3	14.06	1.031	88.5	90	r
Cedrene-V6	13.054	0.935	87.1	88.4	t
globulol	20.527	0.825	71.6	78.3	a3
6-methyl-2,4-di-tert-butyl-phenol	20.125	0.823	91.8	93.2	a2
1-(allyloxy)-4-tert-butylbenzene	13.297	0.792	80.9	87.5	u
alpha-gurjunene	14.523	0.735	77.8	82.7	w
β-caryophyllene	17.625	0.712	90.1	95.1	l
β-caryophyllene	15.953	0.66	83.3	86.1	l
Isolongifolene-5-ol	10.505	0.571	81.2	83.6	q
beta-neoclovene	13.899	0.508	87.5	89.9	v
cis-*beta*-ocimene	9.586	0.505	94	96.7	o
Thujopsene-I3	12.439	0.483	88.5	90.5	r
2,4-di-tert-butylphenol	23.165	0.467	90.3	93.2	a4
1R-*alpha*-pinene	9.284	0.422	91.6	96.2	i
τ-gurjunene	15.594	0.333	85.6	88.5	y
(+)-valencene	18.704	0.327	93	94	m
beta-pinene	8.036	0.277	90.3	95.9	a
geranyl acetate	18.892	0.228	85.9	92.5	a1
(+)-Longifolene	16.312	0.195	83.4	87.8	z

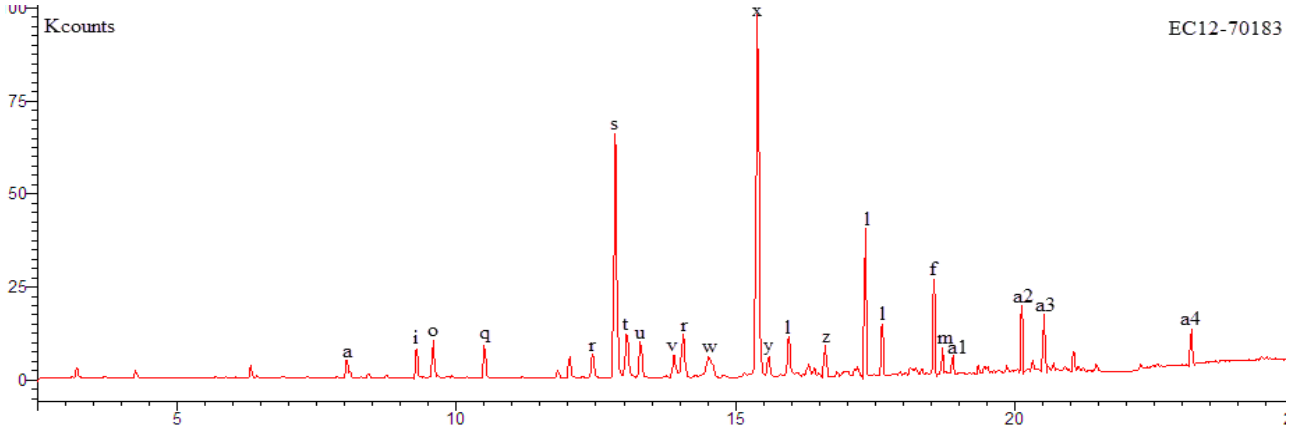

Table S4:

YH40-80361 on Amino Acids					
Compound	Retention Time (min)	% total peak area	Match (%)	R-match (%)	Peak ID
β-chamigrene	18.543	0.832	89.2	90.4	f
β-caryophyllene	17.315	0.464	93.2	93.5	l
(+)-valencene	18.7	0.382	93.1	94.5	m
2,4-Di-tert-butylphenol	23.157	0.28	87.8	91	a4
Limonene	8.764	0.097	83.1	90.6	b

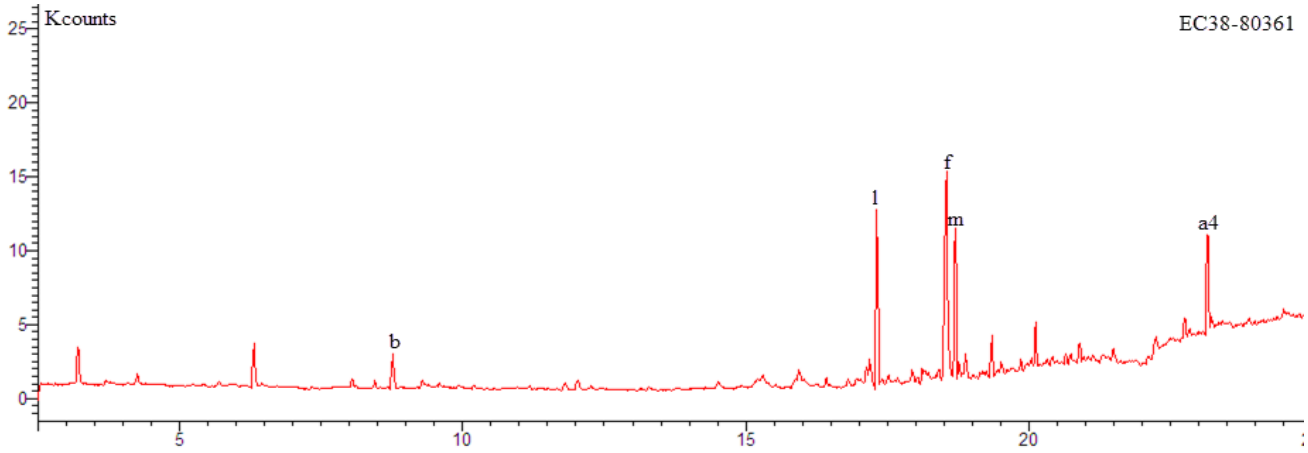

Table S5:

YH40-24646 on Amino Acids					
Compound	Retention Time (min)	% total peak area	Match (%)	R-match (%)	Peak ID
τ-gurjunene	18.111	17.055	89.5	89.6	y
α-gurjunene	17.145	2.29	90.9	91.2	a5
τ-elemene	18.853	1.557	91.9	92.4	a6
beta-pinene	8.054	1.482	94.8	95.4	a
cis-*beta*-ocimene	9.596	1.359	96.3	96.7	o
1S-*alpha*-pinene	9.295	0.943	93.7	96.5	I
β-chamigrene	18.547	0.863	89.2	90.6	F
α-gurjunene	17.891	0.842	92.1	94.4	a5
α-gurjunene	17.589	0.66	93.7	95.7	a5
Butylated hydroxytoluene	20.119	0.435	89.8	92.2	n
2,4-Di-tert-butylphenol	23.161	0.416	92.2	94.6	a4
τ-gurjunene	17.459	0.352	91.3	94.3	y

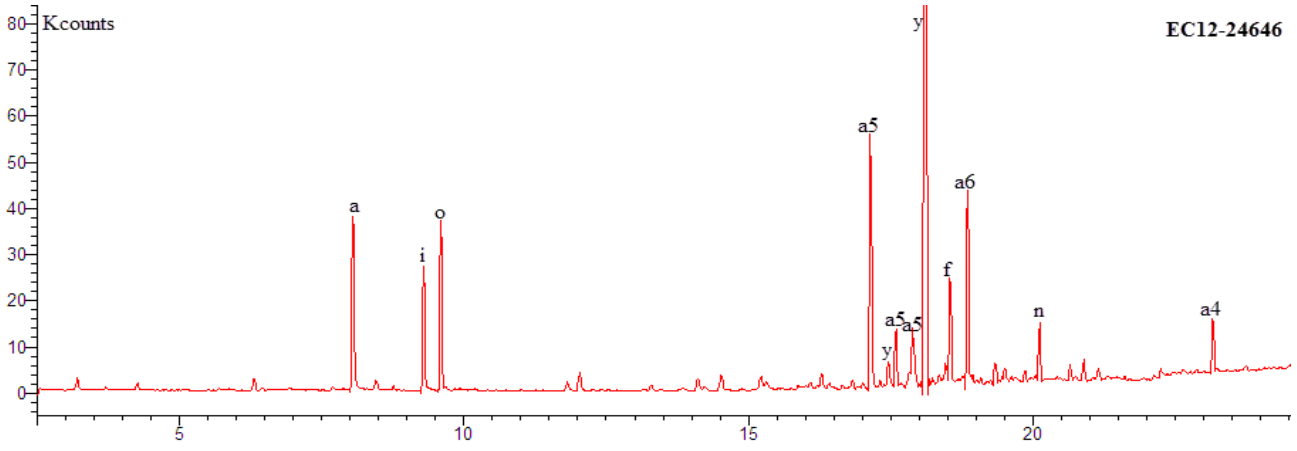

Table S6:

YH40-6706 on Amino Acids					
Compound	Retention Time (min)	% total peak area	Match (%)	R-match (%)	Peak ID
alpha-gurjunene	14.264	12.082	88.2	89.3	a5
Caryophyllene-(I1)	14.815	10.418	88.1	88.8	b1
Longifolene-(V4)	14.554	8.853	90.8	91.5	z
(-)-alpha-gurjunene	15.664	4.076	94.2	94.7	a5
beta-maaliene	12.764	3.763	88.2	88.8	a7
(-)-alloaromadendrene	17.283	3.654	92.8	93.7	b3
beta-caryophyllene	15.228	3.601	93.9	94.7	l
2-Isopropenyl-4a,8-dimethyl-1,2,3,4,4a,5,6,7-octahydronaphthalene	13.354	3.387	90	90.3	a8
alpha-selinene	22.629	3.092	89	91.1	b5
alpha-gurjunene	12.494	2.601	89.2	90	a5
beta-pinene	8.061	2.294	95	95.7	a
alpha-selinene	18.973	2.214	90.7	92.8	b5
(+)-Longifolene	15.353	2.111	80.8	81.7	z
5beta,7beta-H,10alpha-eudesm-11-en-1alpha-ol	19.986	1.906	85.3	87	b7
2-Tridecanone	19.294	1.702	92.4	93.7	b6
beta-chamigrene	18.508	1.272	89.8	90.2	f
Thujopsene-(I2)	13.662	1.236	88.6	91	a9
(+)-Valencene	18.66	1.23	94.7	95.8	m
Limonene	8.773	1.22	91.8	93	c
(-)-alloaromadendrene	17.469	1.191	92.9	94.1	b3
Thujopsene-(I2)	16.184	1.163	83.5	85.3	a9
Thujopsene-I3	12.413	0.954	89.5	90.9	r
alpha-humulene	18.176	0.835	89.8	95.9	b4
beta-caryophyllene	18.256	0.787	93.2	95.3	l
1S-alpha-pinene	9.294	0.749	91.6	96.9	i
(+)-Valencene	17.019	0.661	88.6	93	m
1,2,3,6-Tetramethylbicyclo[2.2.2]octa-2,5-diene	16.011	0.576	78.5	89.3	b2
beta-cis-ocimene	9.594	0.436	90.6	95.9	o
(-)-alloaromadendrene	16.934	0.361	86.6	92.3	b3
1R-alpha-pinene	5.458	0.272	84.6	95.6	j

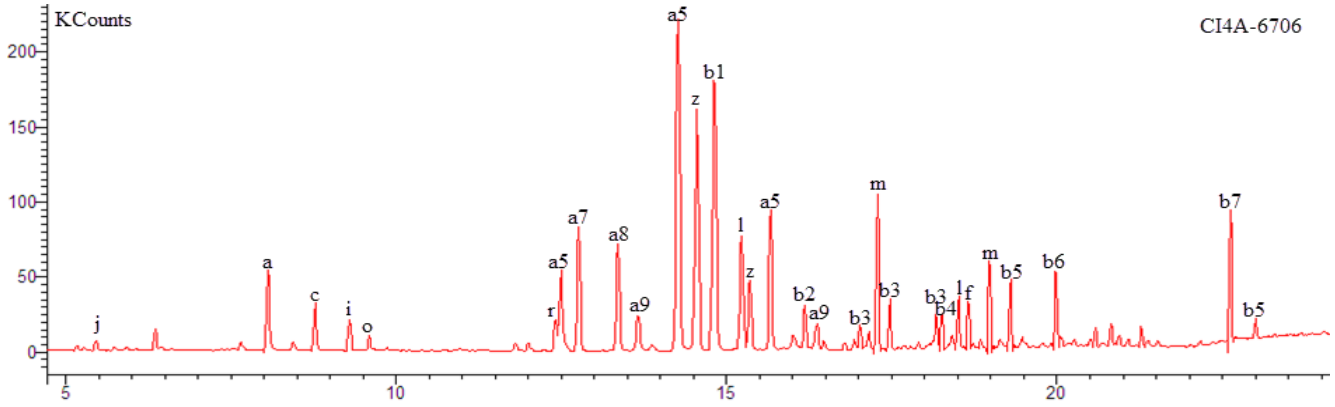
KCounts
CI4A-6706
200
150
100
50
0
5
10
15
20
j
a
c
i
o
r
a5
a7
a8
a9
a5
b1
z
l
z
a5
b2
a9
b3
m
b3
b3
b4
f
m
b5
b6
b7
b5

Reference

1. M. Z. Jacobson, *Energy and Environment Science*, 2009, **2**, 148–173.
2. A. A. Davis R, Pienkos PT, *Applied Energy*, 2011, **88**, 3524-3531.
3. n. Bobban Subhadra a, MarkEdwards, *Energy Policy*, 2010, **38**, 4897-4902.
4. M. P. D. Stuart A Scott, John S Dennis, Irmtraud Horst, Christopher J Howe, David J Lea-Smith and Alison G Smith, *Current Opinion in Biotechnology* 2010, **21**, 277-286.
5. K. K. Sharma, H. Schuhmann and P. M. Schenk, *Energies*, 2012, **5**, 1532-1553.
6. R. W. Davis, J. V. Volponi, H. D. Jones, B. J. Carvalho, H. Wu and S. Singh, *Biotechnol Bioeng*, 2012, **109**, 2503-2512.
7. C. Adams, V. Godfrey, B. Wahlen, L. Seefeldt and B. Bugbee, *Bioresour Technol*, 2013, **131**, 188-194.
8. E. W. Becker, *Microalgae: Biotechnology and Microbiology*, Cambridge University Press, New York, NY, 1994.
9. J. Singh and S. Cu, *Renewable & Sustainable Energy Reviews*, 2010, **14**, 2596-2610.
10. R. Luque, *Energy and Environmental Science*, 2010, **3**, 254–257.
11. M. Martin and I. E. Grossmann, *Applied Energy*, 2014, **135**, 108-114.
12. V. de la Cruz, S. Hernandez, M. Martin and I. E. Grossmann, *Industrial & Engineering Chemistry Research*, 2014, **53**, 14397-14407.
13. S. H. Sharma KK, Schenk PM .*Energies* 2012, 1532-1553.
14. P. Fasahati, H. C. Woo and J. J. Liu, *Applied Energy*, 2015, **139**, 175-187.
15. L. Kexun, L. Shun and L. Xianhua, *International Journal of Energy Research*, 2014, **38**, 965-977.
16. R. Babujanarthanam and P. Kavitha, *Energy Sources Part a-Recovery Utilization and Environmental Effects*, 2014, **36**, 1305-1314.
17. *Marine Pollution Bulletin*, 2011, **62**, 658-658.
18. H. M. El-Mashad, *Biochemical Engineering Journal*, 2015, **93**, 119-127.
19. C. J. Chen Y, Creamer KS, *Bioresource technology* 2008, **99**, 4044-4064.
20. R. Razeghifard, *Photosynthesis Research*, 2013, **117**, 207-219.
21. Y.-X. Huo, K. M. Cho, J. G. L. Rivera, E. Monte, C. R. Shen, Y. Yan and J. C. Liao, *Nature biotechnology*, 2011, **29**, 346-U160.
22. P. P. Peralta-Yahya, F. Zhang, S. B. del Cardayre and J. D. Keasling, *Nature*, 2012, **488**, 320-328.
23. C. Nakano, H.-K. Kim and Y. Ohnishi, *Chembiochem*, 2011, **12**, 1988-1991.
24. http://www1.eere.energy.gov/bioenergy/pdfs/algal_biofuels_roadmap.pdf.
25. A. T. Rufino, M. Ribeiro, C. Sousa, F. Judas, L. Salgueiro, C. Cavaleiro and A. F. Mendes, *European journal of pharmacology*, 2015, **750C**, 141-150.
26. A. L. Klauke, I. Racz, B. Pradier, A. Markert, A. M. Zimmer, J. Gertsch and A. Zimmer, *European Neuropsychopharmacology*, 2014, **24**, 608-620.
27. L. Han, L. Yang, B. Liu and X. Cheng, *European Food Research and Technology*, 2014, **239**, 1061-1066.
28. H. Liu, Z. Song, D. Liao, T. Zhang, F. Liu, K. Zhuang, K. Luo and L. Yang, *Neurochemical Research*, 2015, **40**, 118-123.
29. L. I. G. Paula-Freire, M. L. Andersen, V. S. Gama, G. R. Molska and E. L. A. Carlini, *Phytomedicine*, 2014, **21**, 356-362.
30. R. Singh, *Org. Process Res. Dev.*, 2011, **15**, 175-179.
31. W. H. Adey, P. C. Kangas and W. Mulbry, *BioScience*, 2011, **61**, 434-441.
32. H. M. Miziorko, *Archives of Biochemistry and Biophysics*, 2011, **505**, 131-143.
33. J. R. Anthony, L. C. Anthony, F. Nowroozi, G. Kwon, J. D. Newman and J. D. Keasling, *Metabolic Engineering*, 2009, **11**, 13-19.
34. J. Maury, M. A. Asadollahi, K. Moller, M. Schalk, A. Clark, L. R. Formenti and J. Nielsen, *Febs Letters*, 2008, **582**, 4032-4038.
35. D. J. Pitera, C. J. Paddon, J. D. Newman and J. D. Keasling, *Metabolic Engineering*, 2007, **9**, 193-207.
36. F. Rohdich, S. Hecht, A. Bacher and W. Eisenreich, *Pure and Applied Chemistry*, 2003, **75**, 393-405.

37. F. Rohdich, S. Hecht, K. Gartner, P. Adam, C. Krieger, S. Amslinger, D. Arigoni, A. Bacher and W. Eisenreich, *Proceedings of the National Academy of Sciences of the United States of America*, 2002, **99**, 1158-1163.
38. S. Amslinger, K. Kis, S. Hecht, P. Adam, F. Rohdich, D. Arigoni, A. Bacher and W. Eisenreich, *Journal of Organic Chemistry*, 2002, **67**, 4590-4594.
39. C. A. T. AM Gladden, Connie Gao, Greg O'Bryan, Amy J Powell, Adam M Scheer, Kevin Turner, Weihua Wu, Eizadora T Yu, *Sandia Report*, 2013, 2013-10094.
40. X. Huang, Y. Xiao, T. G. Koellner, W. Zhang, J. Wu, J. Wu, Y. Guo and Y. Zhang, *Plant Physiology and Biochemistry*, 2013, **73**, 302-308.
41. V. J. J. Martin, D. J. Pitera, S. T. Withers, J. D. Newman and J. D. Keasling, *Nature biotechnology*, 2003, **21**, 796-802.
42. W. Wu and Z. Fan, *Bioprocess and Biosystems Engineering*, 2013, **36**, 1631-1640.
43. L. J. Weaver, M. M. L. Sousa, G. Wang, E. Baidoo, C. J. Petzold and J. D. Keasling, *Biotechnology and Bioengineering*, 2015, **112**, 111-119.
44. J. W. Moody, C. M. McGinty and J. C. Quinn, *Proceedings of the National Academy of Sciences of the United States of America*, 2014, **111**, 8691-8696.
45. H.-W. Yen, I. C. Hu, C.-Y. Chen, S.-H. Ho, D.-J. Lee and J.-S. Chang, *Bioresource Technology*, 2013, **135**, 166-174.
46. http://www.biofuelsdigest.com/bdigest/2014/06/18/9-advanced-molecules-that-could-revolutionize-jet-and-missile-fuel/.
47. G. Strobel, *Current Opinion in Microbiology*, 2014, **19**, 52-58.
48. G. A. Strobel, B. Knighton, K. Kluck, Y. Ren, T. Livinghouse, M. Griffin, D. Spakowicz and J. Sears, *Microbiology-Sgm*, 2010, **156**, 3830-3833.
49. M. A. Griffin, D. J. Spakowicz, T. A. Gianoulis and S. A. Strobel, *Microbiology-Sgm*, 2010, **156**, 3814-3829.
50. G. A. Strobel, B. Knighton, K. Kluck, Y. Ren, T. Livinghouse, M. Griffin, D. Spakowicz and J. Sears, *Microbiology-Sgm*, 2008, **154**, 3319-3328.
51. T. Grawert, M. Groll, F. Rohdich, A. Bacher and W. Eisenreich, *Cell Mol Life Sci*, 2011, **68**, 3797-3814.
52. T. S. Lee, R. Chan, S. W. Kim and J. D. Keasling, *Abstracts of Papers of the American Chemical Society*, 2010, **239**.
53. V. Illarionova, J. Kaiser, E. Ostrozhenkova, A. Bacher, M. Fischer, W. Eisenreich and F. Rohdich, *Journal of Organic Chemistry*, 2006, **71**, 8824-8834.
54. S. W. Kim and J. D. Keasling, *Biotechnology and Bioengineering*, 2001, **72**, 408-415.
55. S. M. Ma, D. E. Garcia, A. M. Redding-Johanson, G. D. Friedland, R. Chan, T. S. Batth, J. R. Haliburton, D. Chivian, J. D. Keasling, C. J. Petzold, T. S. Lee and S. R. Chhabra, *Metabolic Engineering*, 2011, **13**, 588-597.
56. T. S. Lee, R. A. Krupa, F. Zhang, M. Hajimorad, W. J. Holtz, N. Prasad, S. K. Lee and J. D. Keasling, *Journal of Biological Engineering*, 2011, **5**.
57. J. C. Anderson, J. E. Dueber, M. Leguia, G. C. Wu, J. A. Goler, A. P. Arkin and J. D. Keasling, *Journal of Biological Engineering*, 2010, **4**, 1-1.
58. G. L. R. a. E. A. Ceccarelli, *Frontiers in Microbiology*, 2014, **5**, 1-17.
59. D. J. Miller and R. K. Allemann, *Natural Product Reports*, 2012, **29**, 60-71.
60. E. Oldfield and F.-Y. Lin, *Angewandte Chemie-International Edition*, 2012, **51**, 1124-1137.
61. J. Degenhardt, T. G. Koellner and J. Gershenzon, *Phytochemistry*, 2009, **70**, 1621-1637.
62. R. Croteau and D. E. Cane, *Methods in Enzymology*, 1985, **110**, 383-405.
63. J. Alonso-Gutierrez, R. Chan, T. S. Batth, P. D. Adams, J. D. Keasling, C. J. Petzold and T. S. Lee, *Metabolic Engineering*, 2013, **19**, 33-41.
64. https://salis.psu.edu/software/
65. W. Weihua, *International Journal of Agricultural and Biological Engineering*, 2013, **6**, 42-53.
66. S. Rodriguez, J. Kirby, C. M. Denby and J. D. Keasling, *Nature Protocols*, 2014, **9**, 1980-1996.